



Nonlinear optical properties of MoS₂-WS₂ heterostructure in fiber lasers

W. J. LIU,^{1,2} M. L. LIU,¹ B. LIU,¹ R. G. QUHE,¹ M. LEI,^{1,3} S. B. FANG,² H. TENG,² AND Z. Y. WEI^{2,*}

¹State Key Laboratory of Information Photonics and Optical Communications, School of Science, P. O. Box 122, Beijing University of Posts and Telecommunications, Beijing 100876, China

²Beijing National Laboratory for Condensed Matter Physics, Institute of Physics, Chinese Academy of Sciences, Beijing 100190, China

³mlei@bupt.edu.cn

*zywei@iphy.ac.cn

Abstract: As a saturable absorption material, the heterostructure with the van der Waals structure has been paid much attention in material science. In general, the heterogeneous combination is able to neutralize, or even exceed, the individual material's advantages in some aspects. In this paper, which describes the magnetron sputtering deposition method, the tapered fiber is coated by the MoS₂-WS₂ heterostructure, and the MoS₂-WS₂ heterostructure saturable absorber (SA) is fabricated. The modulation depth of the prepared MoS₂-WS₂ heterostructure SA is measured to be 19.12%. Besides, the theoretical calculations for the band gap and carrier mobility of the MoS₂-WS₂ heterostructure are provided. By employing the prepared SA, a stable and passively erbium-doped fiber laser is implemented. The generated pulse duration of 154 fs is certified to be the shortest among all fiber lasers based on transition metal dichalcogenides. Results in this paper provide the new direction for the fabrication of ultrafast photon modulation devices.

© 2019 Optical Society of America under the terms of the [OSA Open Access Publishing Agreement](#)

1. Introduction

Since the emergence of graphene [1–4], a variety of two-dimensional (2D) materials, such as topological insulators [5–7], black phosphorus (BP) [8–10] and some new materials [11–13], have sprung up rapidly and occupied an important position in the field of optoelectronics. As effective optical modulation materials, 2D materials can be employed in fiber lasers to generate ultrashort pulses [14,15]. As a result, they have attracted increasing attention in recent years.

Transition metal dichalcogenides (TMDs), which are considered to be the supplements or even the substitutes of graphene in some cases, have also been investigated in the field effect transistors, photocatalysts, photodetectors and optical modulators [16–29]. WS₂ and MoS₂, as two representative materials of TMDs, have been fully explored from the physical to optoelectronic properties. The nonlinear optical response of MoS₂ which is stronger than graphene at 800 nm has been investigated by using Z-scan technique [30]. Then, the broadband saturable absorption of MoS₂ has been illustrated by theoretical arithmetic and further successfully demonstrated at 1.06 μm, 1.42 μm and 2.1 μm [31]. As the analogue of MoS₂, WS₂ not only has good performance in ultra-wide response, but also exhibits a large second-order nonlinear susceptibility [32]. Therefore, WS₂ has great potential in realizing ultrashort pulses. Both MoS₂ and WS₂ perform well as optical modulation materials in fiber lasers.

As far as we know, molecular layers of TMDs are connected by van der Waals (vdW) forces. The weak vdW forces between two adjacent TMD layers not only enable them easier to be stripped into monolayer nanosheets, but also provide a chance to manufacture optoelectronic devices by stacking different TMDs without considering the problem of

mismatch [33,34]. The structure of heterostructure opens up a different avenue for the fabrication of better photoelectric devices. From previous reports, the MoS₂-WS₂ heterostructure exhibits remarkable performances. The type-II semiconductor heterostructures came from stacked MoS₂-WS₂ heterostructure facilitate the transfer of holes [35,36]. Moreover, the absorption of MoS₂-WS₂ heterostructure is larger than the simple superposition of the respective absorptions of MoS₂ and WS₂ [37]. Therefore, the heterostructure consisting of two different materials with various geometric composition and electronic energy exhibits unique electrical and optical properties [38–40]. However, the MoS₂-WS₂ heterostructure SA is rarely used in the fiber lasers for ultrafast photonics. As far as we know, only Chen et al. has made an attempt at the application of the WS₂-MoS₂-WS₂ heterostructure in the fiber laser so far [41].

Among the various preparation methods, the magnetron sputtering deposition (MSD) method with the simple operation is considered to be the most suitable method for the preparation of MoS₂-WS₂ heterostructure with high quality in this paper. MoS₂ and WS₂ are coated on the tapered fibers to manufacture the MoS₂-WS₂ heterostructure SA. Herein, the fiber laser is implemented to investigate the related nonlinear optical performance of the proposed MoS₂-WS₂ heterostructure SA. After the application of SA in fiber laser, a stable mode-locking system is obtained. The obtained pulse duration of 154 fs is proved to be the shortest in the congeneric fiber lasers. The theoretical and experimental results illustrate that the MoS₂-WS₂ heterostructure provides reference value for the innovation and development of fiber lasers.

2. Result and discussion

2.1 Theoretical calculation of MoS₂-WS₂ heterostructure SA

By the density functional theory (DFT) implemented in the Vienna *ab initio* simulation package (VASP), the theoretical calculations were performed. The interactions between valence electrons and core electrons were described with the projector augmented wave (PAW) pseudopotential. A cutoff energy was chosen to be 420 eV for the plane-wave expansion of wave functions. For the integration over the first Brillouin zone, the Monkhorst-Pack scheme of the k-point sampling was adopted. In order to avoid the interactions between two slabs in the nearest-neighbor unit cells, the periodic boundary conditions and a vacuum space of 30 Å along the z direction were applied. A 7 × 7 × 1 grid for the k-point sampling was used for the geometry optimization, while 37 × 37 × 1 was used for the static total energy calculations. When the change of the total energy was less than 10⁻⁴ eV, the forces became smaller than 0.01 eV/Å, the structure began to relax. The calculated lattice constant of monolayer MoS₂, monolayer WS₂ and MoS₂-WS₂ heterostructures are 3.160 Å, 3.153 Å and 3.160 Å, respectively.

The mobility μ of the MoS₂-WS₂ heterostructure was calculated using the deformation potential (DP) theory on the basis of the effective mass approximation:

$$\mu = \frac{2e\hbar^3 C}{3k_B T |m^*|^2 E^2}, \quad (1)$$

where T is the temperature, and C is the elastic modulus. For the 2D system, the in-plane value is defined as $C^{2D} = [\partial^2 E / \partial \delta^2] / S_0$, where E , δ , and S_0 are the total energy, applied uniaxial strain and area of the investigated system, respectively. The DP constant E along a certain direction is obtained by $E = dE_{edge} / d\delta$, where E_{edge} is the energy of the band edges (valence-band maximum for holes, and conduction-band minimum for electrons).

The heterostructure was modeled by a MoS₂-WS₂ bilayer structure in Fig. 1(a). To get the most stable structure, the heterostructure of the strain WS₂ monolayer was used, and the corresponding lattice mismatch is 0.15%. The band gap of the MoS₂-WS₂ heterostructure is 1.26 eV, which is smaller than the band gap of the monolayer MoS₂ (1.77 eV) shown in Fig. 1. The effective mass of electrons and the effective mass of holes in K are 0.46 m_0 and 0.72 m_0 , respectively. The effective mass of holes is smaller than that of the monolayer MoS₂, and the effective mass of electrons is almost equal to the monolayer MoS₂.

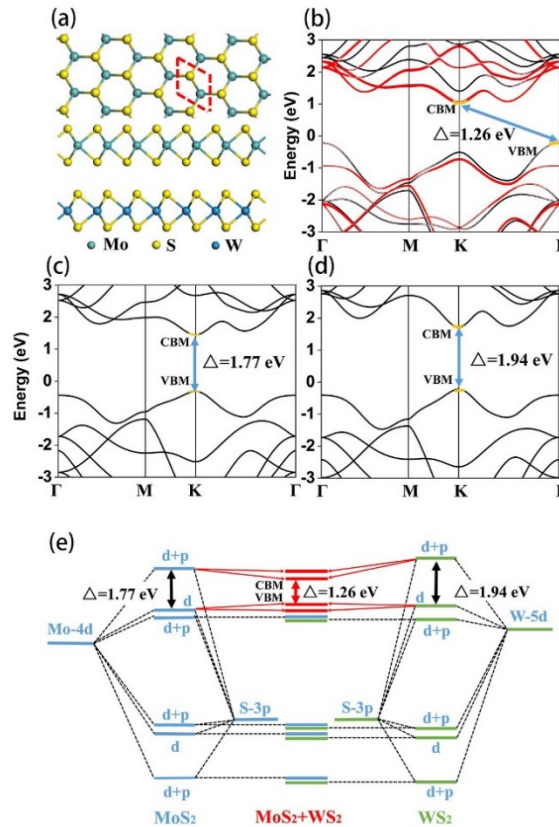


Fig. 1. Atomic and electronic structure of the MoS₂-WS₂ heterostructure. (a) Top and side views of the MoS₂-WS₂ heterostructure, the dashed rectangle denotes the primitive cell. (b), (c) and (d) are band structures of MoS₂-WS₂ heterostructure, monolayer MoS₂ and monolayer WS₂, respectively. Here, the fermi level is set to be zero, and the orange line denotes valence-band maximum for the holes and conduction-band minimum for the electrons. Besides, red points project the contribution from the MoS₂ in (b). (e) is the band alignment of the MoS₂-WS₂ heterostructure. The energy levels of MoS₂ and monolayer WS₂ slabs are shown in both sides. Here, the monolayer MoS₂, monolayer WS₂, and MoS₂-WS₂ heterostructure are considered.

Table 1. Band Gap (E_g), Effective Mass and Carrier Mobility (μ) of Monolayer and Heterostructure Materials

Units	Band gap type	E_g (eV)	Carrier type	Effective mass(m_0)	μ (cm ² ·V ⁻¹ ·s ⁻¹)
MoS ₂	direct	1.77	e	0.46	108.31
			h	0.60	658.19
WS ₂	direct	1.94	e	0.31	221.64

			h	0.40	2865.11
MoS ₂ -WS ₂	indirect	1.26	e	0.46	155.77
			h	0.72	887.39

The effective mass and carrier mobility of the MoS₂-WS₂ heterostructure, monolayer MoS₂ and WS₂ are shown in Table 1. The carrier mobility of the MoS₂-WS₂ heterostructure is larger than that of the monolayer MoS₂. These results may be related to the type-II heterostructure from the stacked MoS₂-WS₂ heterostructure. Specifically, upon optical excitation, the electron tends to stay in the MoS₂ layer which reside with the minimum conduction band, and the holes prefer to stay in the WS₂ layer which reside with the maximum valence band. Therefore, the type-II heterostructure effectively assist electrons and holes separate quickly. The relationship between relaxation time ($\langle \tau \rangle$) and electron mobility (μ_{2D}) can be calculated as $\mu_{2D} = \frac{e \langle \tau \rangle}{m}$, where m is the effective mass. As far as we know, the large relaxation time can bring about greater modulation depth. Therefore, in the same case, the greater the product of effective mass (m) and electron mobility (μ_{2D}), the higher the modulation depth.

2.2 Fabrication and characterization of MoS₂-WS₂ heterostructure SA

The MoS₂-WS₂ heterostructure SA was prepared by the MSD method. Before deposition, the surface impurities of the WS₂ and MoS₂ raw materials were removed, which guaranteed the purity of materials produced. During deposition, the MoS₂ target and taper fiber were placed in the vacuum chamber at the same time, and the pressure of the cavity was set to be 1.7×10^{-3} pa. The Ar gas was continuously excited under the 0.4 A alternating current (AC) with voltage of 6 V for 70 s. Following, WS₂ nanosheets were deposited on the surface of MoS₂ in the same way under the 0.5 A with voltage of 6 V for 180 s. Finally, a dense layer of gold film, which prevents the material from being damaged oxidized, was deposited on the surface of the MoS₂-WS₂ heterostructure.

To characterize the surface and lateral properties of the MoS₂-WS₂ heterostructure SA, the scanning electron microscope (SEM) was employed. Figure 2(a) exhibits the surface morphology of the SA. We can observe that the particles are arranged in a compact and uniform manner. As shown in Fig. 2(b), the lateral surface illustrates the thickness of the heterostructure. To ensure accuracy, the thickness of the sample is measured in three different places. The average value of three different places which is calculated as 63 nm illustrates the thickness of MoS₂-WS₂ heterostructure. According to measuring results, the thickness of MoS₂ is 21 nm and the thickness of WS₂ is 42 nm. The thickness of the SiO₂ substrate is measured to be 59 nm. Those results prove that the obtained MoS₂-WS₂ has layered structure.

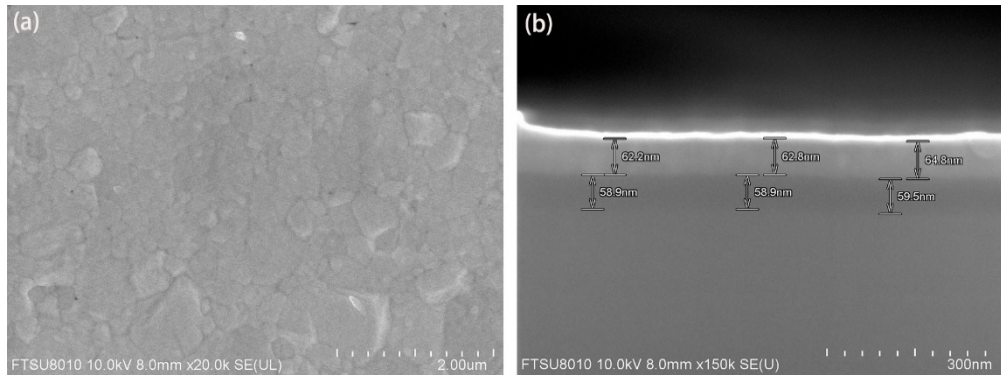


Fig. 2. SEM of the MoS₂-WS₂ heterostructure SA. (a) The surface morphology; (b) The thickness of heterostructure indicated by the lateral.

Raman analysis is a common method to distinguish the types of materials through different vibration modes. In order to confirm the successful manufacture of the MoS₂-WS₂ heterostructure SA, the corresponding Raman spectra are measured in Fig. 3(a). The measurements show that the Raman spectra of the pure MoS₂ sample have peaks at 378 cm⁻¹ and 404 cm⁻¹, which correspond to the E_{2g} and A_{1g}, respectively [42]. The peaks at 355 cm⁻¹ and 419 cm⁻¹ in Raman spectra of WS₂ is corresponding to E_{2g}¹ and A_{1g} modes [34]. The four peaks shown in the Raman spectra of the MoS₂-WS₂ heterostructure are in good agreement with the four vibration modes of MoS₂ and WS₂. The nonlinear absorption properties of the MoS₂-WS₂ heterostructure SA are investigated by the balanced twin-detector method. In the measurement, the mode-locked fiber laser with the repetition rate of 135 MHz and pulse duration of 100 fs is used as the exciting source. The measurement results in Fig. 3(b) demonstrate that the prepared MoS₂-WS₂ heterostructure SA has the modulation depth of 19.12%. Moreover, the saturation absorption intensity of 1.361 MW/cm² is relatively small, which is beneficial to the low self-starting threshold for the fiber laser. The optical damage threshold of the current absorber device is calculated to be 4.17 mJ/cm², which is higher than the commercial available semiconductor saturable absorber mirrors (SESAMs) (500 μJ/cm²).

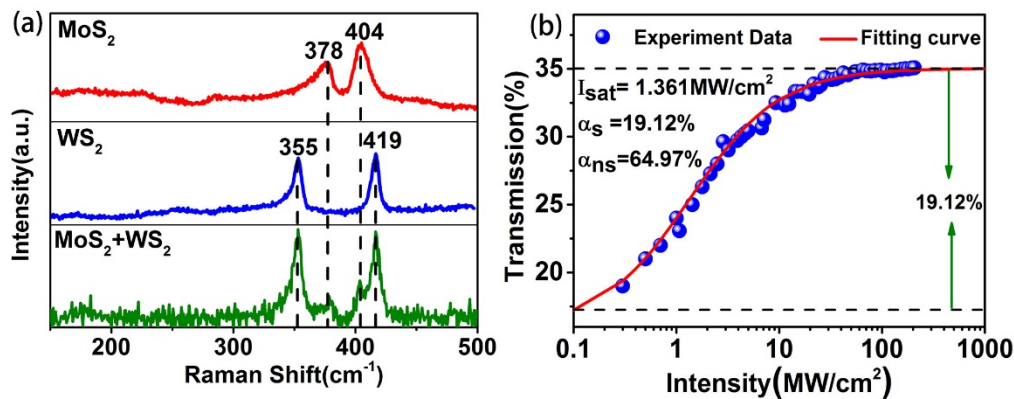


Fig. 3. (a) The Raman spectra of the MoS₂, WS₂ and MoS₂-WS₂ heterostructure; (b) The nonlinear absorption of the MoS₂-WS₂ heterostructure SA.

3. Nonlinear optical performance

To investigate the nonlinear absorption characteristics of the MoS₂-WS₂ heterostructure SA, it has been integrated into the erbium-doped fiber (EDF) laser in Fig. 4. The wavelength division multiplexer (WDM) (980/1550 nm) coupled the pump light into the ring cavity. With the excitation of the pump which operated at 976 nm, a piece of EDF of 42 cm amplified the

pulse through the energy level transition. The polarization controller (PC) was used to fine tune the polarization state and birefringence in the cavity. In order to avoid reflecting light damage to the device, isolator (ISO) enforced light to transmit in a fixed direction. The starting threshold of the laser was 180 mW. When the pump power was greater than this value, the laser maintained the stable mode-locking operation. Through the 20:80 optical coupler (OC), the experimental results were displayed and recorded. The main test instruments we adopted were a 250 MHz oscilloscope and spectrum analyzer.

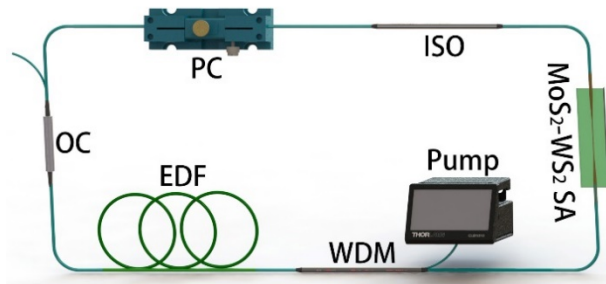


Fig. 4. Experimental device diagram of the passively mode-locked EDF laser employed with the MoS₂-WS₂ heterostructure SA.

Figure 5 summarizes the laser performance at the maximum pump power of 630 mW. As indicated in Fig. 5(a), the central optical spectrum is located at 1560 nm with 3 dB spectral width of 24.4 nm. From the symmetrical Kelly sidebands of the spectrum, it can be inferred that this is the soliton mode locking system. The regular array of the pulse train in Fig. 5(b) indicates that the mode-locked system is in a stable operative condition. The time interval of two neighboring pulses is 13.4 ns, which is corresponding to the fundamental repetition rate 74.6 MHz of mode-locked pulses. The resolution bandwidth (RBW) and span adopted in the measurement of the fundamental frequency are 10 Hz and 10 kHz, respectively. Under high resolution and small span, there is no obvious frequency interference signals appear, and the signal-to-noise ratio (SNR) is 91.2 dB in Fig. 5(c), which further illustrate that the mode-locked operation is relatively stable. Moreover, the pulses in the illustration of Fig. 5(c) are in the uniform arrangement. The symmetrical autocorrelation trace is fitted by the Sech^2 function in Fig. 5(d), which indicates that pulse duration of the mode-locked fiber laser is 154 fs. The corresponding time-bandwidth product (TBP) is 0.4403, indicating that the output mode-locked pulses are slightly chirped. The maximum output power of the laser is 19.8 mW. Results demonstrate that the MoS₂-WS₂ heterostructure SA shows the saturable absorption property around 1.5 μm . According to previous reports, the direct bandgap of the monolayer MoS₂ is 1.8 eV, and the indirect bandgap of the bulk MoS₂ is 1.29 eV. Obviously, the photon energy is below the optical (excitonic) bandgap of MoS₂ at 1560 nm in our work. Although the governing mechanism is still unclear, there have been several convincing theories put forward by researchers, such as multiphoton absorption, edge state saturable absorption and defect state saturable absorption [43]. In the theory of defect state, the imperfection of the 2D material is inevitable in the production process, which has an impact both on its electronic and optical properties [44]. Wang et al. has demonstrated that the MoS₂ bandgap can be reduced from 1.08 to 0.08 eV by introducing the defects in a suitable range. By the introduction of S defects, the MoS₂ has been successfully applied in fiber lasers at the operating wavelength of 1.06, 1.42, and 2.1 μm [45]. Therefore, it is justified to believe that there are unavoidable defects in the material, which result in the decrease of the band gap and broadband absorption beyond expectation.

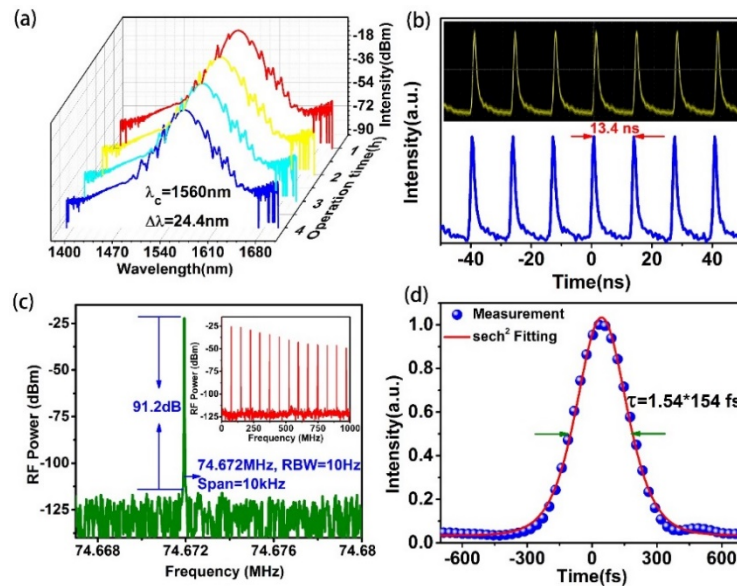


Fig. 5. The performance of the passively mode-locked EDF laser employed with the MoS₂-WS₂ heterostructure SA. (a) The optical spectrum located at 1560 nm with 3 dB spectral width of 24.4 nm; (b) The mode-locked pulse train; (c) The radio-frequency spectrum; (d) The symmetrical autocorrelation trace of mode-locked pulses.

To prove the long-term stability of new SA device, the continuous monitoring for output power of the fiber laser is implemented in Fig. 6. The total monitoring time was up to 16 hours, and the output power of the fiber laser was recorded every second. As shown in Fig. 6, the standard deviation of the output power is only 0.123. This result indicates that the system has good stability. Limited by the experimental conditions, we only monitored the output power within 16 hours, but it can be observed that the trend of data remained stable in the later period, which indicated that the system could maintain stability for a longer time. Therefore, the new SA device can withstand long-term illumination.

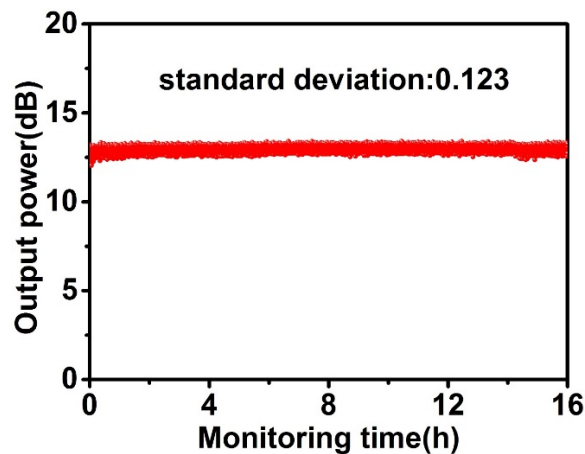


Fig. 6. The continuous monitoring of output power of the fiber laser.

To illustrate the relative advantages and improvements of the proposed mode-locked EDF laser based on the MoS₂-WS₂ heterostructure SA, the performance of mode-locked fiber lasers employed with pure TMDs materials are compared in Table 2. Although there have been some researches on the electronic properties and nonlinear characteristics of the

monolayer MoS₂ (or WS₂), almost all MoS₂ (or WS₂) that applied in mode-locked fiber lasers are multilayered according to the previous reports. Because the preparation of the highly efficient SA based on monolayer material is complicated and difficult. The pulse duration obtained is 154 fs, which is almost the shortest among the similar fiber lasers. Considering the structural particularity of the MoS₂-WS₂ heterostructure, we think there are two reasons for the remarkable performance of the fiber laser: Firstly, the ultrafast transfer time of carriers from the type-II semiconductor heterostructures may be beneficial to the generation of ultrashort pulses. For the monolayer MoS₂, the intra-layer carrier recombination time is 2 ps [41]. However, it has been reported that the electronic transfer in the MoS₂-WS₂ heterostructure occurs within 50 fs upon photo-excitation [35]. Compared with MoS₂ itself, the carrier recombination of the MoS₂-WS₂ heterostructure is much faster. Moreover, we can see that no matter what the thickness of the material is, the pulse duration of the corresponding laser is not as short as that of the fiber laser based on the MoS₂-WS₂ heterostructure in Table 2. The above results give us reason to believe that the vertically stacking of WS₂ and MoS₂ may cause ultrafast carrier recombination, which further benefits the generation of ultrashort pulses. Secondly, the large modulation depth of the MoS₂-WS₂ heterostructure SA is also propitious to the generation of ultrashort pulses. On the one hand, compared with the pure TMDs materials, the combination of the nonlinear absorption properties of two materials makes it more advantageous in the modulation of light. It has been reported that the absorption of the MoS₂-WS₂ heterostructure is larger than the simple superposition of the respective absorptions of MoS₂ and WS₂ in previous works [40]. On the other hand, the tapered fiber structure of the MoS₂-WS₂ heterostructure SA enhances its nonlinearity. The tapered fiber allows a very long interaction length. In commonly used sandwich structures, the interaction length of the material and light is limited by the thickness of the material, often in the nanoscale. However, in the tapered fiber, the interaction length can be extended to centimeter magnitude order by means of the evanescent field effect. This sufficient reaction of the material and light enables the material to fully exhibit its nonlinearity. Besides, SAs based on tapered fibers with different specifications show differences in the modulation depth, and SAs with small waist diameter tend to show larger modulation depth. Therefore, we believe that the tapered fiber structure of the MoS₂-WS₂ heterostructure SA can enhance its nonlinearity.

Table 2. Comparisons of Mode-Locked Fiber Lasers Employed with Different SAs

Materials	Thickness	Pulse duration (ps)	Modulation depth (%)	SNR (dB)	Output power (mW)	Refs.
Graphene	–	0.088	11	65	1.5	[46]
Bi ₂ Se ₃	–	0.66	3.9	55	1.8	[47]
Sb ₂ Te ₃	40-100	1.8	–	60	0.5	[48]
BP	–	0.946	8.1	70	–	[49]
WS ₂	1 μm	0.395	7.8	64	1.5	[50]
	3L	0.595	2.9	75	–	[51]
	5-6nm	0.369	0.6	69	1.93	[52]
	25nm	>0.22	6.5	–	–	[53]
	160nm	0.675	1.2	67	0.625	[54]
	9-16nm	21.1	5.1	<70	1.8	[55]
MoS ₂	30nm	0.84	1.5	57.9	0.034	[56]
	4-5L	3	2.82	–	5.39	[57]
	1-3L	800	9.3	50	9.3	[58]
	1-3L	656	10.47	59	2.37	[59]
	7nm	0.637	2.5	61	–	[60]
WSe ₂	5-6L	0.606	2.7	97	5.9	[61]
	23.9 μm	1.25	0.5	–	0.45	[62]
MoSe ₂	2-3nm	1.45	0.63	61.5	0.44	[63]
	30 μm	0.798	5.4	59.1	22.8	[64]
MoTe ₂	2.5nm	1.2	1.8	–	–	[43]
WTe ₂	80-150nm	0.77	2.85	67	0.04	[65]

WS ₂ -MoS ₂ -WS ₂	132.3nm	0.296	16.99	90.3	25	[38]
MoS ₂ -WS ₂	63nm	0.154	19.12	91.2	19.8	This work

4. Conclusions

In this paper, we have prepared the MoS₂-WS₂ heterostructure SA using the MSD method. The modulation depth and saturation absorption intensity of the SA is 19.12% and 1.361 MW/cm², respectively. The corresponding band gap and electron mobility have been theoretically calculated. In order to investigate the nonlinear absorption characteristics of the MoS₂-WS₂ heterostructure SA, it has been integrated into the EDF laser. In addition, the stable mode-locked fiber laser operating at 1560 nm with SNR of 91.2 dB and output power of 19.8 mW has been implemented. The obtained pulse duration of 154 fs has been proved to be the shortest in the congeneric fiber lasers. Results in this paper not only reveal the impressive optical nonlinearity of the MoS₂-WS₂ heterostructure SA, but also provide reference value for the application and development of TMDs heterostructures.

Funding

National Natural Science Foundation of China (11674036, 11875008); Beijing Youth Top-Notch Talent Support Program (2017000026833ZK08); State Key Laboratory of Information Photonics and Optical Communications (IPOC2017ZZ05).

References

1. A. K. Geim and K. S. Novoselov, "The rise of graphene," *Nat. Mater.* **6**(3), 183–191 (2007).
2. F. Bonaccorso, Z. Sun, T. Hasan, and A. C. Ferrari, "Graphene photonics and optoelectronics," *Nat. Photonics* **4**(9), 611–622 (2010).
3. Q. Bao, H. Zhang, B. Wang, Z. Ni, C. H. Y. X. Lim, Y. Wang, D. Y. Tang, and K. P. Loh, "Broadband graphene polarizer," *Nat. Photonics* **5**(7), 411–415 (2011).
4. Z. T. Wang, Y. Chen, C. J. Zhao, H. Zhang, and S. C. Wen, "Switchable dual-wavelength synchronously Q-switched erbium-doped fiber laser based on graphene saturable absorber," *IEEE Photonics J.* **4**(3), 869–876 (2012).
5. W. Liu, L. Pang, H. Han, W. Tian, H. Chen, M. Lei, P. Yan, and Z. Wei, "70-fs mode-locked erbium-doped fiber laser with topological insulator," *Sci. Rep.* **6**(1), 19997 (2016).
6. Y. H. Lin, S. F. Lin, Y. C. Chi, C. L. Wu, C. H. Cheng, W. H. Tseng, J. H. He, C. I. Wu, C. K. Lee, and G. R. Lin, "Using n- and p-Type Bi₂Te₃ topological insulator nanoparticles to enable controlled femtosecond mode-locking of fiber lasers," *ACS Photonics* **2**(4), 481–490 (2015).
7. J. Ma, S. Lu, Z. Guo, X. Xu, H. Zhang, D. Tang, and D. Fan, "Few-layer black phosphorus based saturable absorber mirror for pulsed solid-state lasers," *Opt. Express* **23**(17), 22643–22648 (2015).
8. F. Xia, H. Wang, and Y. Jia, "Rediscovering black phosphorus as an anisotropic layered material for optoelectronics and electronics," *Nat. Commun.* **5**(1), 4458 (2014).
9. H. R. Mu, S. H. Lin, Z. C. Wang, S. Xiao, P. F. Li, Y. Chen, H. Zhang, H. F. Bao, S. P. Lau, C. X. Pan, D. Y. Fan, and Q. L. Bao, "Pulsed lasers: black phosphorus-polymer composites for pulsed lasers," *Adv. Opt. Mater.* **3**(10), 1447–1453 (2015).
10. J. Li, H. Luo, B. Zhai, R. Lu, Z. Guo, H. Zhang, and Y. Liu, "Black phosphorus: a two-dimension saturable absorption material for mid-infrared Q-switched and mode-locked fiber lasers," *Sci. Rep.* **6**(1), 30361 (2016).
11. Y. H. Xu, Z. T. Wang, Z. N. Guo, H. Huang, Q. L. Xiao, H. Zhang, and X.-F. Yu, "Solvochemical synthesis and ultrafast photonics of black phosphorus quantum dots," *Adv. Opt. Mater.* **4**(8), 1223–1229 (2016).
12. X. T. Jiang, S. X. Liu, W. Y. Liang, S. J. Luo, Z. L. He, Y. Q. Ge, H. D. Wang, R. Cao, F. Zhang, Q. Wen, J. Q. Li, Q. L. Bao, D. Y. Fan, and H. Zhang, "Broadband nonlinear photonics in few-layer MXene Ti₃C₂T_x (T= F, O, or OH)," *Laser Photonics Rev.* **12**(2), 1700229 (2018).
13. L. Lu, Z. M. Liang, L. M. Wu, Y. X. Chen, Y. F. Song, S. C. Dhanabalan, J. S. Ponraj, B. Q. Dong, Y. J. Xiang, F. Xing, D. Y. Fan, and H. Zhang, "Few-layer bismuthene: sonochemical exfoliation, nonlinear optics and applications for ultrafast photonics with enhanced stability," *Laser Photonics Rev.* **12**(1), 1700221 (2018).
14. Q. H. Wang, K. Kalantar-Zadeh, A. Kis, J. N. Coleman, and M. S. Strano, "Electronics and optoelectronics of two-dimensional transition metal dichalcogenides," *Nat. Nanotechnol.* **7**(11), 699–712 (2012).
15. F. N. Xia, H. Wang, D. Xiao, M. Dubey, and A. Ramasubramaniam, "Two-dimensional material nanophotonics," *Nat. Photonics* **8**(12), 899–907 (2014).
16. J. Baek, D. M. Yin, N. Liu, I. Omkaram, C. Jung, H. Im, S. Hong, S. M. Kim, Y. K. Hong, J. Hur, Y. Yoon, and S. Kim, "A highly sensitive chemical gas detecting transistor based on highly crystalline CVD-grown MoSe₂ films," *Nano Res.* **10**(6), 1861–1871 (2017).

17. W. J. Liu, M. L. Liu, M. Lei, S. B. Fang, and Z. Y. Wei, "Titanium selenide saturable absorber mirror for passive Q-switched Er-doped fiber laser," *IEEE J. Sel. Top. Quant.* **24**(3), 1 (2018).
18. J. A. Wilson and A. D. Yoffe, "The transition metal dichalcogenides discussion and interpretation of the observed optical, electrical and structural properties," *Adv. Phys.* **18**(73), 193–335 (1969).
19. W. Liu, M. Liu, Y. OuYang, H. Hou, G. Ma, M. Lei, and Z. Wei, "Tungsten diselenide for mode-locked erbium-doped fiber lasers with short pulse duration," *Nanotechnology* **29**(17), 174002 (2018).
20. F. Schwier, J. Pezoldt, and R. Granzner, "Two-dimensional materials and their prospects in transistor electronics," *Nanoscale* **7**(18), 8261–8283 (2015).
21. W. Liu, M. Liu, J. Yin, H. Chen, W. Lu, S. Fang, H. Teng, M. Lei, P. Yan, and Z. Wei, "Tungsten diselenide for all-fiber lasers with the chemical vapor deposition method," *Nanoscale* **10**(17), 7971–7977 (2018).
22. J. Yin, H. Chen, W. Lu, M. Liu, I. Ling Li, M. Zhang, W. Zhang, J. Wang, Z. Xu, P. Yan, W. Liu, and S. Ruan, "Large-area and highly crystalline MoSe₂ for optical modulator," *Nanotechnology* **28**(48), 484001 (2017).
23. M. L. Liu, Y.-Y. OuYang, H.-R. Hou, M. Lei, W.-J. Liu, and Z.-Y. Wei, "MoS₂ saturable absorber prepared by chemical vapor deposition method for nonlinear control in Q-switching fiber laser," *Chin. Phys. B* **27**(8), 084211 (2018).
24. W. J. Liu, M. L. Liu, H. N. Han, S. B. Fang, H. Teng, M. Lei, and Z. Y. Wei, "Nonlinear optical properties of WSe₂ and MoSe₂ films and their applications in passively Q-switched erbium doped fiber lasers," *Photon. Res.* **6**(10), C15–C21 (2018).
25. W. Liu, M. Liu, Y. OuYang, H. Hou, M. Lei, and Z. Wei, "CVD-grown MoSe₂ with high modulation depth for ultrafast mode-locked erbium-doped fiber laser," *Nanotechnology* **29**(39), 394002 (2018).
26. W. Y. Li, Y. OuYang, G. Ma, M. Liu, and W. Liu, "Q-switched all-fiber laser with short pulse duration based on tungsten diselenide," *Laser Phys.* **28**(5), 055104 (2018).
27. K. Wang, J. Wang, J. Fan, M. Lotya, A. O'Neill, D. Fox, Y. Feng, X. Zhang, B. Jiang, Q. Zhao, H. Zhang, J. N. Coleman, L. Zhang, and W. J. Blau, "Ultrafast saturable absorption of two-dimensional MoS₂ nanosheets," *ACS Nano* **7**(10), 9260–9267 (2013).
28. Y. Li, N. Dong, S. Zhang, X. Zhang, Y. Feng, K. Wang, L. Zhang, and J. Wang, "Giant two-photon absorption in monolayer MoS₂," *Laser Photonics Rev.* **9**(4), 427–434 (2015).
29. X. Zhang, S. Zhang, B. Chen, H. Wang, K. Wu, Y. Chen, J. Fan, S. Qi, X. Cui, L. Zhang, and J. Wang, "Direct synthesis of large-scale hierarchical MoS₂ films nanostructured with orthogonally oriented vertically and horizontally aligned layers," *Nanoscale* **8**(1), 431–439 (2016).
30. K. Wang, J. Wang, J. Fan, M. Lotya, A. O'Neill, D. Fox, Y. Feng, X. Zhang, B. Jiang, Q. Zhao, H. Zhang, J. N. Coleman, L. Zhang, and W. J. Blau, "Ultrafast saturable absorption of two-dimensional MoS₂ nanosheets," *ACS Nano* **7**(10), 9260–9267 (2013).
31. S. Wang, H. Yu, H. Zhang, A. Wang, M. Zhao, Y. Chen, L. Mei, and J. Wang, "Broadband few-layer MoS₂ saturable absorbers," *Adv. Mater.* **26**(21), 3538–3544 (2014).
32. C. Janisch, Y. Wang, D. Ma, N. Mehta, A. L. Elias, N. Perea-López, M. Terrones, V. Crespi, and Z. Liu, "Extraordinary second harmonic generation in tungsten disulfide monolayers," *Sci. Rep.* **4**(1), 5530 (2015).
33. J. Kang, H. Sahin, and F. M. Peeters, "Tuning carrier confinement in MoS₂/WS₂ lateral heterostructure," *J. Phys. Chem. C* **119**(17), 9580–9586 (2015).
34. J. Zhang, J. Wang, P. Chen, Y. Sun, S. Wu, Z. Jia, X. Lu, H. Yu, W. Chen, J. Zhu, G. Xie, R. Yang, D. Shi, X. Xu, J. Xiang, K. Liu, and G. Zhang, "Observation of strong interlayer coupling in MoS₂/WS₂ heterostructures," *Adv. Mater.* **28**(10), 1950–1956 (2016).
35. X. Hong, J. Kim, S. F. Shi, Y. Zhang, C. Jin, Y. Sun, S. Tongay, J. Wu, Y. Zhang, and F. Wang, "Ultrafast charge transfer in atomically thin MoS₂/WS₂ heterostructures," *Nat. Nanotechnol.* **9**(9), 682–686 (2014).
36. N. J. Huo, J. Kang, Z. M. Wei, S. S. Li, J. B. Li, and S. H. Wei, "Novel and enhanced optoelectronic performances of multilayer MoS₂-WS₂ heterostructure transistors," *Adv. Funct. Mater.* **24**(44), 7025–7031 (2014).
37. Y. Yu, S. Hu, L. Su, L. Huang, Y. Liu, Z. Jin, A. A. Purezky, D. B. Geohegan, K. W. Kim, Y. Zhang, and L. Cao, "Equally efficient interlayer exciton relaxation and improved absorption in epitaxial and nonepitaxial MoS₂/WS₂ heterostructures," *Nano Lett.* **15**(1), 486–491 (2015).
38. G. H. Han, J. A. Rodríguez-Manzo, C. W. Lee, N. J. Kybert, M. B. Lerner, Z. J. Qi, E. N. Dattoli, A. M. Rappe, M. Drndic, and A. T. Johnson, "Continuous growth of hexagonal graphene and boron nitride in-plane heterostructures by atmospheric pressure chemical vapor deposition," *ACS Nano* **7**(11), 10129–10138 (2013).
39. A. Mishchenko, J. S. Tu, Y. Cao, R. V. Gorbachev, J. R. Wallbank, M. T. Greenaway, V. E. Morozov, S. V. Morozov, M. J. Zhu, S. L. Wong, F. Withers, C. R. Woods, Y. J. Kim, K. Watanabe, T. Taniguchi, E. E. Vdovin, O. Makarovskiy, T. M. Fromhold, V. I. Fal'ko, A. K. Geim, L. Eaves, and K. S. Novoselov, "Twist-controlled resonant tunnelling in graphene/boron nitride/graphene heterostructures," *Nat. Nanotechnol.* **9**(10), 808–813 (2014).
40. T. Gao, X. Song, H. Du, Y. Nie, Y. Chen, Q. Ji, J. Sun, Y. Yang, Y. Zhang, and Z. Liu, "Temperature-triggered chemical switching growth of in-plane and vertically stacked graphene-boron nitride heterostructures," *Nat. Commun.* **6**(1), 6835 (2015).
41. H. Chen, J. Yin, J. Yang, X. Zhang, M. Liu, Z. Jiang, J. Wang, Z. Sun, T. Guo, W. Liu, and P. Yan, "Transition-metal dichalcogenides heterostructure saturable absorbers for ultrafast photonics," *Opt. Lett.* **42**(21), 4279–4282 (2017).

42. K. Chen, X. Wan, J. Wen, W. Xie, Z. Kang, X. Zeng, H. Chen, and J. B. Xu, "Electronic properties of MoS₂-WS₂ heterostructures synthesized with two-step lateral epitaxial strategy," *ACS Nano* **9**(10), 9868–9876 (2015).
43. D. Mao, B. Du, D. Yang, S. Zhang, Y. Wang, W. Zhang, X. She, H. Cheng, H. Zeng, and J. Zhao, "Nonlinear saturable absorption of liquid-exfoliated molybdenum/tungsten ditelluride nanosheets," *Small* **12**(11), 1489–1497 (2016).
44. X. Zhang, S. Zhang, Y. Xie, J. Huang, L. Wang, Y. Cui, and J. Wang, "Tailoring the nonlinear optical performance of two-dimensional MoS₂ nanofilms via defect engineering," *Nanoscale* **10**(37), 17924–17932 (2018).
45. S. Wang, H. Yu, H. Zhang, A. Wang, M. Zhao, Y. Chen, L. Mei, and J. Wang, "Broadband few-layer MoS₂ saturable absorbers," *Adv. Mater.* **26**(21), 3538–3544 (2014).
46. J. Sotor, I. Pasternak, A. Krajewska, W. Strupinski, and G. Sobon, "Sub-90 fs a stretched-pulse mode-locked fiber laser based on a graphene saturable absorber," *Opt. Express* **23**(21), 27503–27508 (2015).
47. H. Liu, X. W. Zheng, M. Liu, N. Zhao, A. P. Luo, Z. C. Luo, W. C. Xu, H. Zhang, C. J. Zhao, and S. C. Wen, "Femtosecond pulse generation from a topological insulator mode-locked fiber laser," *Opt. Express* **22**(6), 6868–6873 (2014).
48. J. Sotor, G. Sobon, W. Macherzynski, P. Paletko, K. Grodecki, and K. M. Abramski, "Mode-locking in Er-doped fiber laser based on mechanically exfoliated Sb₂Te₃ saturable absorber," *Opt. Mater. Express* **4**(1), 1–6 (2014).
49. Y. Chen, G. Jiang, S. Chen, Z. Guo, X. Yu, C. Zhao, H. Zhang, Q. Bao, S. Wen, D. Tang, and D. Fan, "Mechanically exfoliated black phosphorus as a new saturable absorber for both Q-switching and Mode-locking laser operation," *Opt. Express* **23**(10), 12823–12833 (2015).
50. H. Chen, L. Li, S. C. Ruan, T. Guo, and P. G. Yan, "Fiber-integrated tungsten disulfide saturable absorber (mirror) for pulsed fiber lasers," *Opt. Eng.* **55**(8), 081318 (2016).
51. K. Wu, X. Zhang, J. Wang, X. Li, and J. Chen, "WS₂ as a saturable absorber for ultrafast photonic applications of mode-locked and Q-switched lasers," *Opt. Express* **23**(9), 11453–11461 (2015).
52. R. Khazaeinezhad, S. H. Kassani, H. Jeong, K. J. Park, B. Y. Kim, D. Yeom, and K. Oh, "Ultrafast pulsed all-fiber laser based on tapered fiber enclosed by few-layer WS₂ nanosheets," *IEEE Photonic. Tech. L.* **27**(15), 1581–1584 (2015).
53. B. Guo, Y. Yao, P. G. Yan, K. Xu, J. J. Liu, S. G. Wang, and Y. Li, "Dual-wavelength soliton mode-locked fiber laser with a WS₂-based fiber taper," *IEEE Photonic. Tech. L.* **28**(3), 323–326 (2016).
54. P. G. Yan, A. J. Liu, Y. S. Chen, H. Chen, S. C. Ruan, C. Y. Guo, S. F. Chen, I. L. Li, H. P. Yang, J. G. Hu, and G. Z. Cao, "Microfiber-based WS₂-film saturable absorber for ultra-fast photonics," *Opt. Mater. Express* **5**(3), 479–489 (2015).
55. D. Mao, S. Zhang, Y. Wang, X. Gan, W. Zhang, T. Mei, Y. Wang, Y. Wang, H. Zeng, and J. Zhao, "WS₂ saturable absorber for dissipative soliton mode locking at 1.06 and 1.55 μm," *Opt. Express* **23**(21), 27509–27519 (2015).
56. J. Lee, J. Park, J. Koo, Y. M. Jhon, and J. H. Lee, "Harmonically mode-locked femtosecond fiber laser using non-uniform, WS₂-particle deposited side-polished fiber," *J. Opt.* **18**(3), 035502 (2016).
57. M. Liu, X. W. Zheng, Y. L. Qi, H. Liu, A. P. Luo, Z. C. Luo, W. C. Xu, C. J. Zhao, and H. Zhang, "Microfiber-based few-layer MoS₂ saturable absorber for 2.5 GHz passively harmonic mode-locked fiber laser," *Opt. Express* **22**(19), 22841–22846 (2014).
58. H. Zhang, S. B. Lu, J. Zheng, J. Du, S. C. Wen, D. Y. Tang, and K. P. Loh, "Molybdenum disulfide (MoS₂) as a broadband saturable absorber for ultra-fast photonics," *Opt. Express* **22**(6), 7249–7260 (2014).
59. J. Du, Q. Wang, G. Jiang, C. Xu, C. Zhao, Y. Xiang, Y. Chen, S. Wen, and H. Zhang, "Ytterbium-doped fiber laser passively mode locked by few-layer Molybdenum Disulfide (MoS₂) saturable absorber functioned with evanescent field interaction," *Sci. Rep.* **4**(1), 6346 (2015).
60. R. Khazaeinezhad, S. H. Kassani, H. Jeong, D. I. Yeom, and K. Oh, "Mode-locking of Er-doped fiber laser using a multilayer MoS₂ thin film as a saturable absorber in both anomalous and normal dispersion regimes," *Opt. Express* **22**(19), 23732–23742 (2014).
61. K. Wu, X. Zhang, J. Wang, and J. Chen, "463-MHz fundamental mode-locked fiber laser based on few-layer MoS₂ saturable absorber," *Opt. Lett.* **40**(7), 1374–1377 (2015).
62. D. Mao, X. She, B. Du, D. Yang, W. Zhang, K. Song, X. Cui, B. Jiang, T. Peng, and J. Zhao, "Erbium-doped fiber laser passively mode locked with few-layer WSe₂/MoSe₂ nanosheets," *Sci. Rep.* **6**(1), 23583 (2016).
63. Z. Q. Luo, Y. Y. Li, M. Zhong, Y. Z. Huang, X. J. Wan, J. Peng, and J. Weng, "Nonlinear optical absorption of few-layer molybdenum diselenide (MoSe₂) for passively mode-locked soliton fiber laser," *Photon. Res.* **3**(3), A79–A86 (2015).
64. J. Koo, J. Park, J. Lee, Y. M. Jhon, and J. H. Lee, "Femtosecond harmonic mode-locking of a fiber laser at 3.27 GHz using a bulk-like, MoSe₂-based saturable absorber," *Opt. Express* **24**(10), 10575–10589 (2016).
65. J. Koo, Y. I. Jhon, J. Park, J. Lee, Y. M. Jhon, and J. H. Lee, "Near-infrared saturable absorption of defective bulk-structured WTe₂ for femtosecond laser mode-locking," *Adv. Funct. Mater.* **26**(41), 7454–7461 (2016).